

Volume and surface mode coupling experiments in periodic surface structures for use in mm-THz high power radiation sources

A. J. MacLachlan,^a C. W. Robertson, A. W. Cross, and A. D. R. Phelps

Department of Physics, SUPA, University of Strathclyde, Glasgow G4 0NG, UK

(Received 23 December 2017; accepted 3 October 2018; published online 12 October 2018)

Planar Periodic Surface Lattice (PSL) structures of different configurations have been designed, fabricated and measured in the 140-220 GHz frequency band. Surface mode resonances are observed in ‘mesh’ PSL structures. We establish that, when mounted on suitable metal-backed dielectric substrates, PSLs exhibit ‘mode-locked’ coherent cavity eigenmodes formed from coupled volume and surface modes. The ‘proof-of-principle’ coupling of volume and surface modes and concept of mode selection in a large cavity, which can lead to the innovation of high power mm-THz radiation sources, is demonstrated. Evidence of coupled eigenmode formation in a 0.64 mm planar PSL measured at 325-500 GHz is presented, verifying the scalability of this work. Excellent agreement between numerical modelling and experiment is reported. © 2018 Author(s). All article content, except where otherwise noted, is licensed under a Creative Commons Attribution (CC BY) license (<http://creativecommons.org/licenses/by/4.0/>). <https://doi.org/10.1063/1.5020542>

Metamaterials, or artificial surfaces, are defined by their exact subwavelength structure and are engineered to exhibit exciting and intriguing phenomena that do not exist in natural materials. Rapidly progressing nanofabrication and subwavelength imaging techniques have led to the emergence of increasingly intricate surface structures at ever shorter wavelengths. Depending on the precise geometry and arrangement of individual subwavelength components, unusual and desirable electromagnetic characteristics such as negative refraction,^{1,2} artificial magnetism and high refractive index,³ can be observed. Exploitation of these unique properties leads to applications in electromagnetic cloaking,⁴ perfect lensing,^{5,6} imaging,^{2,7,8} spectroscopy,⁹ particle acceleration¹⁰ and the development of compact, efficient antennae.¹¹ The manipulation of electromagnetic radiation in subwavelength periodic surfaces is also fundamental to the realisation of novel radiation sources^{12–20} capable of delivering high output powers at high frequencies.

Conventional microwave radiation sources have interaction regions scaled to the source’s intended operating wavelength λ_{op} , limiting the output power at high frequencies. Overcoming this challenge by increasing the cavity dimensions leads to multi-mode operation, detrimental to the efficiency of the device. Here, an innovative mode-coupling technique, involving the coupling of volume and surface fields in large cavities based on ‘effective metadielectric’ Periodic Surface Lattice (PSL) structures (or high-impedance surfaces²¹) is proposed. Experimental validation of this novel mode-selection method, relevant to the realisation of new high power, high frequency radiation sources is presented in this paper.

When mounted on dielectric substrates, the planar PSLs considered in this work, can support both surface and volume fields. Although the lattice corrugation is sufficiently shallow to satisfy the metamaterial criterion, PSLs more closely resemble photonic crystals in the transverse direction, where the lattice period $d_z \sim \lambda_{op}$. While it is possible to develop a high-power radiation source based on a metal planar PSL combined with an electron sheet beam, planar PSLs, especially those mounted on dielectric substrates, are not intended for use within electron-beam-driven sources. Under optimal

^aAuthor to whom correspondence should be addressed: amy.maclachlan@strath.ac.uk

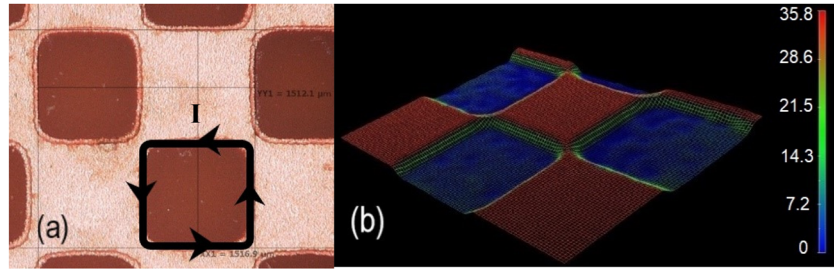


FIG. 1. (a) Photographs of 1.50mm PSL etched onto the 0.76mm substrate, captured using a Hirox microscope. The lighter regions are the copper PSL while the darker areas correspond to dielectric. The arrows show the direction of the induced surface current, I . (b) 3D representation of the shorter wavelength, 0.64mm PSL with corrugation depth $36\mu\text{m}$ and surface roughness $<3\mu\text{m}$.

conditions, the coupling of volume and surface fields on PSLs results in the formation of a high-Q eigenmode. The focus of this work is to experimentally verify the ‘proof-of principle’ coupling of volume and surface modes and establish the necessary conditions for coherent eigenmode formation to occur. Once this volume and surface mode coupling is well understood, planar PSLs can be mapped into cylindrical structures compatible with an electron beam.²⁰

Fig. 1 shows images of planar PSLs captured using a Hirox KH-7700 Digital Microscope. Uniformly etched cells, isolated by well-defined copper boundaries, are observed. When irradiated, an induced surface current flows around each cell, as indicated by the arrows in Fig. 1a, synchronising neighbouring lattice components and facilitating inductive coupling. The induced surface current is scattered into a surface field at the lattice corrugation and interferes with the PSL’s reflected signal, resulting in a well-defined resonance at a particular frequency (f_s) determined by d_z . The volume field contained within the substrate synchronises the individual lattice scatterers and surface fields, required for strong coupling. The 3D representation (fig. 1b) shows the lattice corrugation depth ($36\mu\text{m}$) and surface roughness ($<3\mu\text{m}$) which becomes significant at increasingly shorter wavelengths.

The dispersion relation calculated using the AKS Eigenmode Solver of CST Microwave Studio (CST MWS) in Fig. 2 shows coupled volume and surface fields in a planar PSL with period $d_z = 1.74\text{ mm}$ and corrugation depth $\Delta r = 35\mu\text{m}$, mounted on a 0.76 mm copper-backed substrate. The maxima and minima of these coupled dispersion branches indicate the frequency location of possible coupled eigenmodes. Although the lower dispersion branch (1) coincides with the substrate’s volume field, its flattened appearance (which facilitates ‘mode-locking’) is uncharacteristic of a conventional volume mode and indicates that the surface field is participating in coupling with the volume

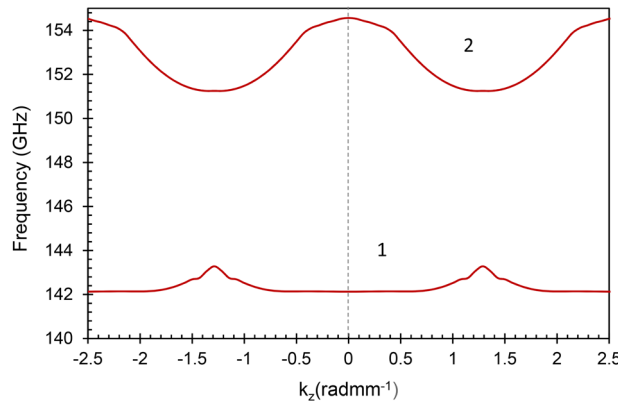


FIG. 2. CST MWS dispersion diagram for $d_z = 1.74\text{ mm}$ PSL with corrugation depth $\Delta r = 35\mu\text{m}$, mounted on 0.76 mm copper-backed substrates with $\epsilon_r = 4.71$. The coupled dispersion branches are formed by coupled volume and surface fields. The maxima and minima of these branches indicate the frequency location of possible coupled eigenmodes.

field at this frequency. Numerical CST MWS dispersion diagrams show good agreement with the theoretical approach detailed in Ref. 22. However, it is important to note that the AKS Eigenmode Solver does not calculate for irradiation angles other than 0° or take into account losses.

Planar PSL structures with $d_z = 1.50$ mm, 1.64 mm, 1.74 mm and 1.94 mm, both with and without dielectric substrates and all with a transverse size of 40 periods, have been designed to operate in the 140-220 GHz frequency band. To extend this research to higher frequencies (325-500 GHz) and prove the structures' scalability, a shorter wavelength, $d_z = 0.64$ mm, PSL is also considered. Both chemical and laser etching techniques were implemented in the fabrication of these structures. PSLs with dielectric substrates were manufactured using a chemical etchant solution to etch copper coated dielectric sheets, with a chosen range of different thicknesses and measured values of permittivity ϵ_r . In certain structures, the copper backing was left intact whilst in others it was entirely dissolved. The copper-backed structures resemble Fabry-Perot cavities, with the lattice and copper backing in place of mirrors.²² Simpler, 0.3 mm thick, copper 'mesh' PSLs, designed to study the surface field exclusively, were obtained via laser etching. Such structures resemble inductive, high band-pass filters²³ and can be likened to an array of rectangular apertures, where the reflected mode lies close to the fundamental $TE_{1,0}$ cut-off frequency. Degenerate modes are neglected due to asymmetries associated with the fabrication process. Higher precision, additive manufacturing^{20,24} can be used to fabricate cylindrical PSL structures with operating frequencies beyond 1 THz. For cylindrical PSLs with \bar{m} azimuthal variations, the surface field couples with a near cut-off $TM_{0,N}$ volume mode to form a hybrid $HE_{\bar{m},1}$ eigenmode. In the planar PSLs, \bar{m} is replaced with \bar{k}_y (where $\bar{k}_y = 2\pi/d_y$ and d_y is the transverse lattice period).

Experimental results were obtained using an Anritsu Vector Star Vector Network Analyzer (VNA) in conjunction with a pair of high frequency OML modules and standard gain (140-220 GHz) horn antennae in free space, as described by MacLachlan²² and photographed in Fig. 3. All measurements were carried out in the Far Field with the horns positioned to illuminate the bulk of the PSL whilst attempting to mitigate undesirable edge effects. The angles of incidence θ_i and reflection θ_r were kept equal ($\theta_i = \theta_r$) with the PSL structure clamped in a fixed position, at the pivot point of the scanning platform's rotating arms ($\theta_i = 0^\circ$).

Surface mode resonances observed in 'mesh' PSLs composed entirely of copper and measured at $\theta_i = 40^\circ$ are presented in Fig. 4(a). A strong angular dependence, where f_s shifts up with increasing θ_i (due to a phase shift between individual lattice components) is shown in Fig. 4(b).

The structures' complexity is increased by introducing a printed circuit board (PCB) substrate of thickness 0.76 mm and $\epsilon_r = 4.71$. In these structures, the PCBs' copper backing was entirely dissolved in the etching process. Additional resonances and complex behaviour are observed for the 1.50 mm PSL (Fig. 5). Inclusion of the lossy dielectric introduces experimental noise and significantly attenuates the field magnitude, particularly at large θ_i . Three distinct resonances are evident in Fig. 5. Higher frequency resonances (2 and 3) are associated with the PSL's surface field, while resonance 1

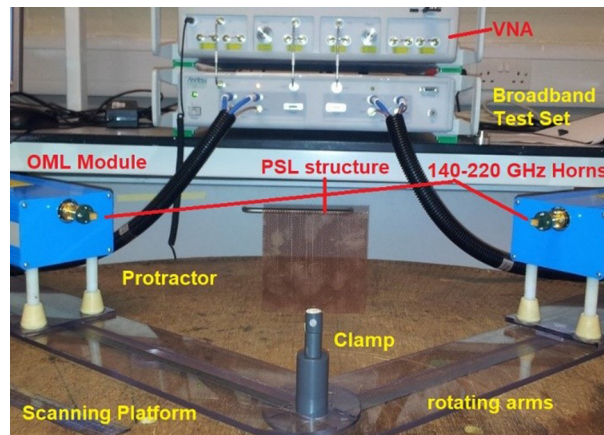


FIG. 3. Photograph showing experimental apparatus and set-up.

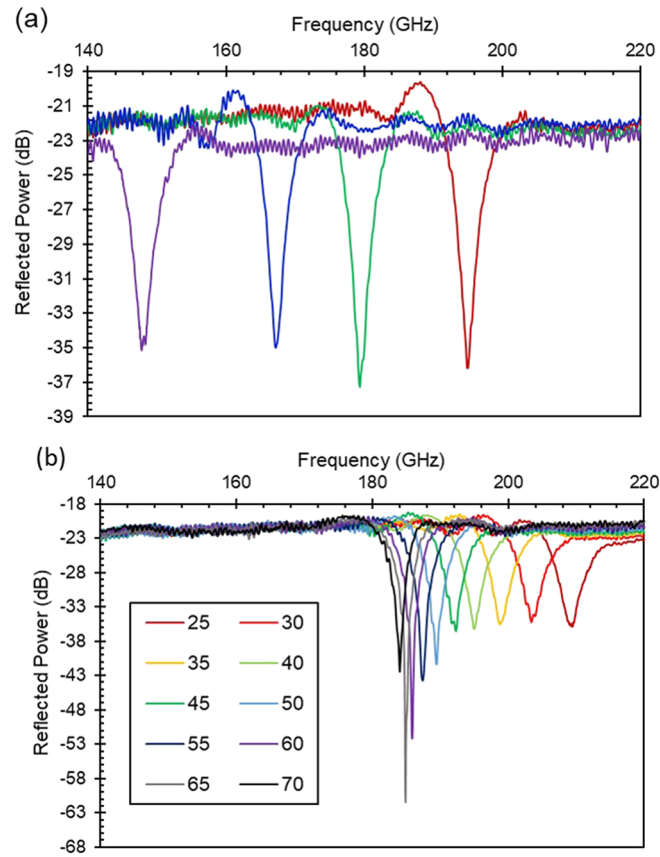


FIG. 4. Reflected surface mode resonances observed in copper ‘mesh’ PSLs without substrates (a) with $d_z = 1.50$ mm (red), 1.62 mm (green), 1.74 mm (blue) and 1.94 mm (purple) observed at $\theta_i = 40^\circ$ (b) $d_z = 1.50$ mm for $\theta_i = 25^\circ$ – 70° . The colors used to denote the various incident angles are shown in the legend.

represents a weak, internally reflected volume mode confined within the dielectric when θ_i exceeds the critical angle, $\theta_c = 26^\circ$.

A similar PSL structure mounted on a thicker 1.43 mm copper-backed PCB substrate, is considered (Fig. 6). In this configuration, the PSL is assembled more like a Fabry-Perot cavity, providing lattice synchronisation.^{19,22} Results presented in Fig. 6 demonstrate that, even with a copper backing plate in place to facilitate strong coupling of volume and surface fields, a suitable substrate must be chosen in order to observe coherent eigenmode formation. Otherwise, multiple resonances, corresponding to weakly coupled volume and surface modes, which are detrimental to the efficiency and mode-selectivity of the cavity, are present.

The large absorptive losses associated with the thicker, 1.43 mm, $\epsilon_r = 4.45$ dielectric impede lattice synchronisation. Resonance 1 describes the volume field confined within the dielectric while 3 and 4 are related to the PSL’s surface field. Resonance 2, which shows no clear angular dependence, is indicative of a weakly coupled cavity eigenmode. Although this resonance is well-defined, particularly at lower θ_i , the maximum reflected signal (~ 39 dB) is significantly weaker than that of Fig. 7(a).

Fig. 7 shows “mode-locked” eigenmode resonances observed in PSLs mounted on 0.76 mm and 0.41 mm copper-backed substrates at 140–220 GHz (Fig. 7a,b) and 325–500 GHz (Fig. 7c) respectively. To achieve this desired, coherent mode-coupling, the PSL must be suitably synchronised, in this case by the volume mode trapped within the dielectric as well as the PSL’s surface current. When a suitable substrate is chosen, the copper backing facilitates synchronisation of the individual lattice scatterers. The shorter wavelength, 0.64 mm PSL mounted on the 0.41 mm copper-backed PCB substrate (Fig. 7c) demonstrates the scalability of this work. Measurements shown in Fig. 7c were made over

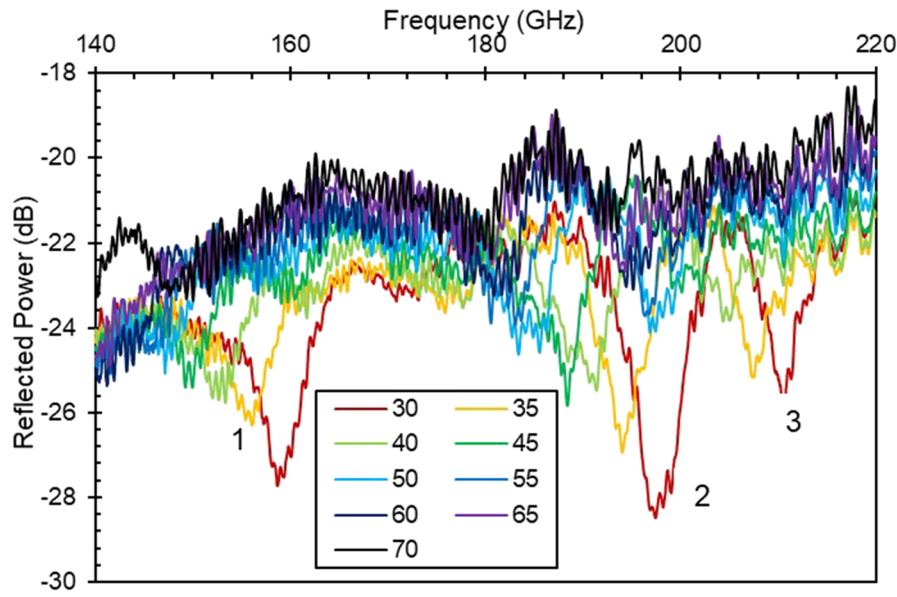


FIG. 5. Reflection measurements at $\theta_i = 30^\circ$ - 70° for the $d_z = 1.50$ mm PSL mounted on a 0.76 mm PCB substrate (without copper backing). The frequency error is ± 0.3 GHz.

a restricted angular range due to the shorter cables required to connect the high frequency modules to the VNA. Precise alignment of the 325-500 GHz antennae required to make these measurements proved difficult and, consequently, the reflected power (~ 5 dB) and therefore quality of the coupled cavity mode, is poor in comparison to the copper-backed PSL structures designed to operate at 140-220 GHz (Fig. 7a,b). Nevertheless, the results presented in Fig. 7c illustrate a coupled, ‘mode-locked’ eigenmode at ~ 371 GHz and show the fundamental “proof of principle” coupling between volume and surface modes, verifying the scalability of these PSLs.

The coupled eigenmode resonances of Fig. 7 dominate over competing behaviour and appear to be ‘mode-locked’ at a particular frequency f_e , irrespective of θ_i . This important phenomenon is observed in all the PSLs mounted on suitable copper-backed substrates.²² ‘Mode-locking’ is most

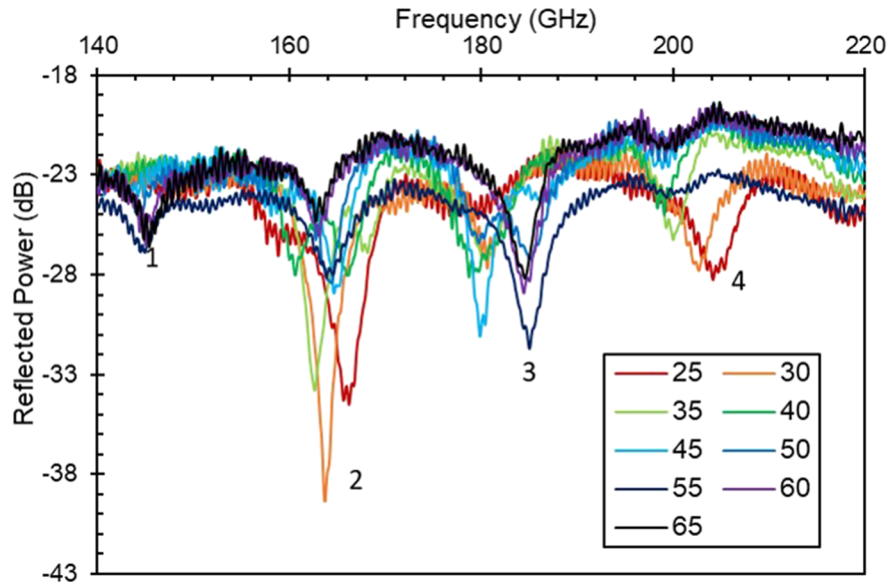


FIG. 6. Reflection measurements for a 1.50 mm PSL mounted on a 1.43 mm copper-backed $\epsilon_r = 4.45$ substrate at $\theta_i = 25^\circ$ - 65° .

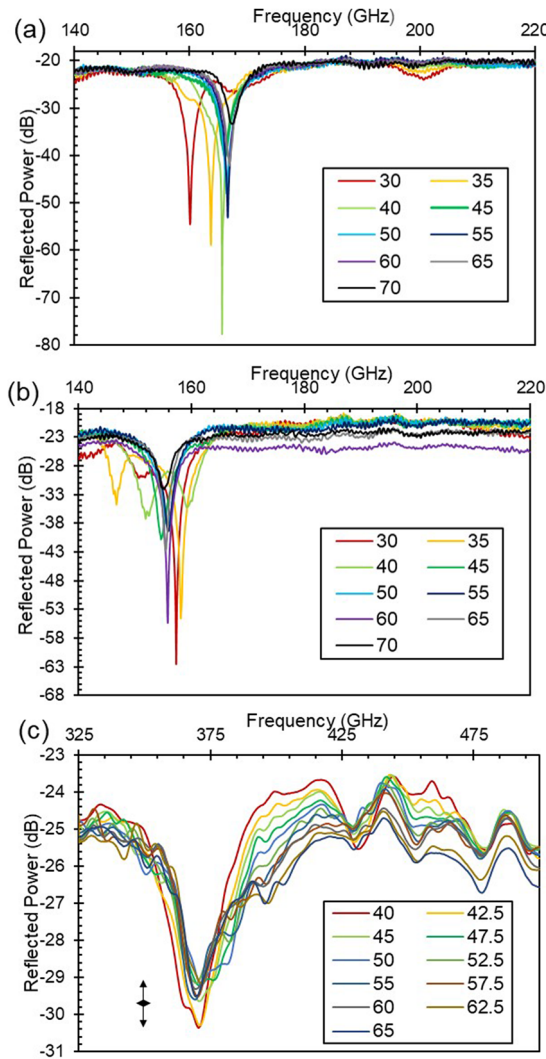


FIG. 7. (a) and (b), coherent, coupled eigenmode formation due to the coupling of volume and surface modes observed for PSLs mounted on 0.76mm, copper-backed, PCB substrates at $\theta_i = 30^\circ$ - 70° . The copper backing enhances lattice synchronisation and facilitates coupling of volume and surface modes. ‘Frequency-locked’ eigenmode resonances are shown for PSLs with (a) $d_z = 1.50$ mm and (b) $d_z = 1.74$ mm. (c) Reflected power for the $d_z = 0.64$ mm PSL mounted on a 0.41 mm copper-backed PCB substrate at $\theta_i = 40^\circ$ - 65° , measured at 325-500 GHz. Coherent, coupled eigenmode formation is observed at ~ 371 GHz. Representative error bar is shown. The magnitude error is ± 0.5 dB and frequency error is ± 0.3 GHz.

effective at higher θ_i , typically $\theta_i > 40^\circ$, suggesting that the larger frequency separation between the volume and surface modes at lower θ_i inhibits coupling. Although some angular dependence is observed in Fig. 7 when $\theta_i < 40^\circ$, the resonances now shift up in frequency with increasing θ_i , indicating that the strong coupling facilitated by the copper backing modifies the electromagnetic response at all angles. Excellent frequency reproducibility (± 0.3 GHz) was reported²⁵ demonstrating the principle of coupled eigenmode formation and mode selection in large cavity structures. Precise alignment is essential for optimum power response and magnitude stability of these measurements.²⁶

Results for the 1.74 mm copper-backed PSL (Fig. 7b) show good agreement with the numerical dispersion diagram of Fig. 2. CST MWS dispersions were calculated for $\theta_i = 0^\circ$ and are therefore best compared to measurements made at low θ_i .²² Three experimental resonances at $\theta_i = 30^\circ$ (fig. 7b) exist within ± 2 GHz of the CST MWS dispersion’s maximum (156 GHz) and minima (144 GHz, 149 GHz) frequencies, while at larger angles ($\theta_i \geq 50^\circ$) the dispersion’s maximum coincides with

TABLE I. Comparison of the experimental results with resonances predicted by the CST MWS Eigenmode Solver.

Lattice period d_z (mm)	Substrate Thickness (mm)	Experimental Resonances (GHz)	CST MWS Eigenmodes (GHz)
0.64	0.41	370 (mode-locked)	360, 372
1.50	0.76	168 (mode-locked)	160, 164, 168
1.94	1.43	142, 151, 157	144, 149, 156

$f_e \sim 156$ GHz. Simulation results for structures with different periodicities and dielectric thicknesses, all mounted on copper-backed substrates, are summarized in Table I and compared with the experimental results. Although the CST MWS dispersion diagrams predict multiple possible eigenmodes for each structure, only one eigenmode exists in the case of mode-locking. In this case, the mode-locked eigenmode corresponds to one of the possible resonances predicted by CST MWS. For the PSL mounted on the thicker, 1.43mm substrate (without mode-locking) all 3 experimental resonances are located within ± 2 GHz of the simulation results. The dispersion diagram of Fig. 2, along with the results reported in Table I, show strong agreement between simulation and experiment.^{22,26}

In conclusion, we have successfully shown volume and surface mode coupling and the formation of high-Q eigenmode resonances in ‘effective metadielectric’ PSLs mounted on copper-backed substrates with appropriate dimensions, therefore demonstrating the structures’ feasibility for use in novel high power radiation sources at high frequencies. ‘Mode-locked’ resonances (which demonstrate the potential for single mode excitation in large cavities) are observed only when the PSL structure is suitably synchronised by the induced surface current and volume mode trapped within the dielectric substrate. The inclusion of the structures’ copper-backing facilitates lattice synchronisation and is one of the conditions required for coherent volume and surface mode coupling. We have established that, even with this copper backing, losses associated with thicker substrates can inhibit lattice synchronisation and are detrimental to coupled eigenmode formation. The manifestation of more than one resonance suggests that the lattice is not ideally synchronised and resonances related to the PSL’s surface field as well as internally reflected volume modes and weakly coupled eigenmodes, have been observed. By studying ‘mesh’ PSLs without substrates it was shown that the surface field frequency is determined by the lattice period, and also influenced by the irradiation angle. Measurements of a shorter wavelength, $d_z = 0.64$ mm PSL mounted on a copper-backed structure, demonstrated volume and surface mode coupling in the 325-500 GHz frequency band, verifying the scalability of this work and showing the structures’ potential to be incorporated into radiation sources at ever higher frequencies. We have demonstrated the fundamental “proof of principle” coupling of volume and surface modes in planar PSLs which, when mapped into cylindrical structures, are suitable for use as the interaction region of new high power coherent radiation sources. Excellent agreement has been obtained between experimental measurements and CST MWS dispersion calculations, allowing structures to be designed to support coupled eigenmodes at desired frequencies. The mode-coupling technique presented in this work is relevant to the realization of radiation sources based on different gain media including vacuum electronic and condensed matter sources.

Useful discussions with Dr. Ivan Konoplev of the John Adams Institute, Department of Physics, University of Oxford, UK are gratefully acknowledged. The authors would like to thank Mr David Barclay for his help making experimental components. This project has received funding from the Leverhulme Trust, United Kingdom, through an International Network Grant IN-2015-012. Amy MacLachlan thanks the EPSRC UK for funding her PhD studentship. This material is based upon work supported by AFOSR under award numbers FA8655-13-1-2132 and FA9550-17-1-0095.

¹ R. A. Shelby, D. R. Smith, and S. Schultz, *Science* **292**, 5514 (2001).

² Z. Lu, J. A. Murakowski, C. A. Schuetz, S. Shi, G. J. Schneider, and D. W. Prather, *Phys. Rev. Lett.* **95**, 153901 (2005).

³ J. T. Shen, P. B. Catrysse, and S. Fan, *Phys. Rev. Lett.* **94**, 197401 (2005).

⁴ D. Schurig, J. J. Mock, B. J. Justice, S. A. Cummer, J. B. Pendry, A. F. Starr, and D. R. Smith, *Science* **314**, 5801 (2006).

⁵ J. B. Pendry, *Phys. Rev. Lett.* **85**, 3966–3969 (2000).

⁶ Z. Liu, N. Fang, T. J. Yen, and X. Zhang, *Appl. Phys. Lett.* **83**, 5184–5186 (2003).

⁷ E. Abraham, A. Younus, A. El. Fatimy, J. C. Delagnes, E. Nguéma, and P. Mounaix, *Opt. Commun.* **282**, 15 (2009).

- ⁸ C. Seco-Martorell, V. López-Domínguez, G. Arauz-Garofalo, A. Redo-Sanchez, J. Palacios, and J. Tejada, *Opt. Exp.* **21**, 15 (2013).
- ⁹ F. Benabid, J. C. Knight, G. Antonopoulos, and P. S. J. Russell, *Science* **298**, 5592 (2002).
- ¹⁰ E. I. Smirnova, A. S. Kesar, I. Mastovsky, M. A. Shapiro, and R. J. Temkin, *Phys. Rev. Lett.* **95**, 074801 (2005).
- ¹¹ S. Shoaib, N. Shoaib, I. Shoaib, and X. Chen, *Micro. Opt. Tech. Lett.* **59**, 148–156 (2017).
- ¹² I. V. Konoplev, L. Fisher, A. W. Cross, A. D. R. Phelps, K. Ronald, and C. W. Robertson, *Appl. Phys. Lett.* **96**, 261101 (2010).
- ¹³ I. V. Konoplev, L. Fisher, A. W. Cross, A. D. R. Phelps, K. Ronald, and M. Thumm, *Appl. Phys. Lett.* **97**, 261102 (2010).
- ¹⁴ I. V. Konoplev, L. Fisher, K. Ronald, A. W. Cross, A. D. R. Phelps, C. W. Robertson, and M. Thumm, *Appl. Phys. Lett.* **96**, 231111 (2010).
- ¹⁵ R. Letizia, M. Mineo, and C. Paoloni, *IEEE Electron Device Lett.* **37**, 1227–1230 (2016).
- ¹⁶ N. S. Ginzburg, A. M. Malkin, A. S. Sergeev, and V. Zaslavsky, *J. Appl. Phys.* **113**, 104504 (2013).
- ¹⁷ C. Paoloni, D. Gamzina, L. Himes, B. Popovic, R. Barchfeld, L. Yue, Y. Zheng, X. Tang, Y. Tang, P. Pan, H. Li, R. Letizia, M. Mineo, J. Feng, and N. C. Luhmann, *IEEE Trans. Plasma Sci.* **44**, 369–376 (2016).
- ¹⁸ I. V. Konoplev, A. J. MacLachlan, C. W. Robertson, A. W. Cross, and A. D. R. Phelps, *Phys. Rev. A* **84**, 013826 (2011).
- ¹⁹ I. V. Konoplev, A. J. MacLachlan, C. W. Robertson, A. W. Cross, and A. D. R. Phelps, *Appl. Phys. Lett.* **101**, 121111 (2012).
- ²⁰ A. R. Phipps, A. J. MacLachlan, C. W. Robertson, L. Zhang, I. V. Konoplev, A. W. Cross, and A. D. R. Phelps, *Nucl. Instrum. Methods Phys. Res. B* **402**, 202–205 (2017).
- ²¹ D. Sievenpiper, L. Zhang, R. F. Jimenez Broas, N. G. Alexöpolous, and E. Yablonovitch, *IEEE Trans. Microwave Theory Tech.* **47**, 2059–2074 (1999).
- ²² A. J. MacLachlan, “Control, manipulation and exploitation of electromagnetic radiation using complex, electrodynamic structures,” PhD Thesis, University of Strathclyde (2015).
- ²³ R. Ulrich, *Appl. Opt.* **7**, 1987–1996 (1968); *Infra. Phys.* **7**, 37–55 (1967).
- ²⁴ D. M. French and D. Shiffler, *Rev. Sci. Instrum.* **87**, 053308 (2016).
- ²⁵ A. J. MacLachlan, A. R. Phipps, C. W. Robertson, A. W. Cross, I. V. Konoplev, and A. D. R. Phelps, UCMMT 2016, 9th UK, Europe, China conference on Millimeter Waves and Terahertz Technologies, Qingdao, China, 5–7 Sept. 2016.
- ²⁶ A. J. MacLachlan *et al.*, data underpinning this publication are available from the University of Strathclyde KnowledgeBase at <http://doi.org/10.15129/dbe44fa1-aa8c-46ec-86fc-10a9ab8791a1>.